

Article

Wood Decay Fungi Associated with Galleries of the Emerald Ash Borer

Sofía Simeto ^{1,2,*} , Benjamin W. Held ¹  and Robert A. Blanchette ¹ 

¹ Department of Plant Pathology, University of Minnesota, 495 Borlaug Hall 1991 Upper Buford Circle, St. Paul, MN 55108, USA

² Programa Nacional de Investigación en Producción Forestal, Instituto Nacional de Investigación Agropecuaria (INIA), Estación Experimental INIA Tacuarembó, Ruta 5 km 386, Tacuarembó 45000, Uruguay

* Correspondence: ssimeto@inia.org.uy

Abstract: The emerald ash borer is causing dramatic losses following its introduction into North America, with hundreds of millions of ash trees killed. Attacked trees lose wood integrity rapidly after infestation and are prone to failure. The aim of this study was to investigate the wood degrading potential of Basidiomycota fungi previously found associated with EAB galleries. Laboratory soil and agar microcosm experiments showed that many of the white-rot fungi isolated were aggressive wood degraders. *Trametes versicolor*, *Phlebia radiata* and *Phlebia acerina* were among the top decomposers from the 13 tested fungi, resulting in as much as 70%, 72% and 64% weight loss, respectively, after 6 months of incubation. Micromorphological observations documented the significant wood cell wall degradation that had taken place. The decay capacity of these fungi confirms their contributing role to the loss of wood integrity in ash trees after EAB attack.

Keywords: emerald ash borer; *Agrilus*; *Fraxinus*; wood decay; fungi; microbial ecology



Citation: Simeto, S.; Held, B.W.; Blanchette, R.A. Wood Decay Fungi Associated with Galleries of the Emerald Ash Borer. *Forests* **2023**, *14*, 576. <https://doi.org/10.3390/f14030576>

Academic Editor: Miha Humar

Received: 19 January 2023

Revised: 2 March 2023

Accepted: 8 March 2023

Published: 14 March 2023



Copyright: © 2023 by the authors. Licensee MDPI, Basel, Switzerland. This article is an open access article distributed under the terms and conditions of the Creative Commons Attribution (CC BY) license (<https://creativecommons.org/licenses/by/4.0/>).

1. Introduction

The emerald ash borer (EAB), *Agrilus planipennis* Fairmaire, is a serious invasive pest causing the extensive mortality of mature ash trees (*Fraxinus* L.) throughout North America, and is considered to have the potential to decimate ash as a component of natural forests. Since its first detection in 2002, it has killed hundreds of millions of ash trees in urban and rural areas, landscapes and forests in North America [1], with significant economic and ecological impact [2–7]. The limited resistance observed among native North American ash species [8–10] results in nearly 100% tree mortality within 3 to 6 years after establishment [11]. Integrated control strategies, such as biological control, monitoring and chemical control, have been used to slow EAB spread and reduce its impact, but efforts to eradicate it have failed. Among the important management efforts that are used to slow the spread of EAB is the prioritized removal of affected trees in urban management plans, as highly infested trees suffer a rapid loss of wood strength and have a higher risk of tree failure, becoming extremely hazardous to people and properties [12].

The EAB life cycle occurs mostly under the bark, where four different larval instars develop while tunnelling characteristic serpentine galleries during one (univoltine) or two (semivoltine) growing seasons [13–15]. This is followed by an overwintering J-shaped prepupa stage that enters diapause until spring, when it molts into a pupa before adult emergence [14–16]. Although EAB adults feed on ash leaves for about two weeks before females start laying eggs [5,10,13], this feeding stage represents no serious damage to the trees. Larvae are the most damaging stage, as they excavate galleries under the bark feeding on the inner phloem, cambium and outer xylem [5,17]. This attack usually begins at canopy level, and canopy decline, dieback and death of branches becomes evident approximately 3–4 years after the initial establishment [5]. During subsequent years, the tree starts to weaken, larval densities increase, and as the tree accumulates galleries on the main trunk

and limbs, water and nutrient transport are critically disrupted and the tree dies [5]. Bark cracks and wounds on branches and stems occur due to larval feeding habits and adults produce exit holes during emergence from the tree. Before tree death takes place, many larval galleries become exposed and subsequent lesions produced by canker, causing fungi associated with EAB attack to be open to the environment [18,19]. Woodpeckers also contribute to exposing galleries, by making holes through the bark when feeding on larvae. All of these wounds and lesions have been hypothesized to potentially act as points of access for fungal spores belonging to several fungal guilds found associated with EAB galleries, such as decay, canker, entomopathogenic and saprotrophic fungi, as reported by Held et al. [18]. It is also possible that some fungi could previously be present as latent endophytes [18,20]. Some of the fungal species associated with EAB galleries, reported by Held et al. [18], were later confirmed as being able to produce canker lesions on healthy young ash trees [19].

The decay fungi reported by Held et al. [18] belong to the Basidiomycota and most of them have been classified as white-rot fungi [18]. Wood decay types traditionally classified as white rot degrade all components of the plant cell wall, including lignin. In contrast, brown-rot fungi depolymerize and degrade cellulose, leaving lignin somewhat altered, but not degraded [21]; whereas, soft-rot fungi produce cavities in the S2 layer of secondary cell walls or may cause secondary cell wall erosion, but little to no degradation of the middle lamella [21–24].

White ash (*Fraxinus americana* L.), black ash (*Fraxinus nigra* Marsh.) and green ash (*Fraxinus pennsylvanica* Marsh.) are considered very sensitive to EAB attack, with green ash regarded as the most susceptible species [25–27]. Additionally, in many localities of the Midwest and Eastern United States, ash trees represent a high percentage of the local tree inventory [6,28]. In Minnesota, although variable among communities, urban ash tree resources average 20% [29,30]. According to Persad et al. [12], green ash is ranked as intermediate in terms of susceptibility to breakage, but there is a significant increased risk of tree and branch failure for ash trees infested by EAB [12]. This poses an additional challenge to EAB management, as EAB-infested trees become very dangerous and must be removed with additional equipment, thus increasing the costs of tree removal and the hazards associated with it. Even though Persad et al. [12] confirmed a higher risk of failure on EAB-attacked trees, the authors did not identify a specific cause to explain the observed loss of structural strength.

Although most of the research on EAB has focused on its biology, impact and management, only a few studies have been published with focus on the fungal community associated with the beetle or its galleries, and the role these fungi have on ash mortality and structural failure of wood [18,19]. Among the decay fungi associated with EAB galleries found by Held et al. (2021) [18], some taxa, such as *Irpex*, *Peniophora* and *Phlebia*, are considered aggressive pioneer white-rot genera, and some other taxa, such as *Ganoderma* and *Trametes*, have been reported as the causal agent of root rot and dieback of woody plants [18,31–33]. However, the ash wood degrading potential of those taxa, including the most abundant strains isolated from ash infested with EAB, has not been determined. The aim of this study was to evaluate the wood degrading potential of thirteen decay fungi isolated from EAB galleries and to evaluate their contributing role in causing hazardous tree conditions following EAB attack on ash trees.

2. Materials and Methods

Decay studies were performed with 13 fungal strains belonging to Basidiomycota, previously obtained and identified by Held et al. (2020) [18] (Table 1). Their wood degrading potential was evaluated in two types of ash wood substrates: ash wood blocks and ash sapwood discs, using two different experimental settings: soil and agar microcosms. Soil-block and agar-block microcosm experiments are the two main methods for studying fungal biodegradation of woody materials under laboratory conditions and both have been originally developed for testing the efficacy of wood preservatives [34–37]. While a

soil-block-standardized protocol has been adopted by the American Society for Testing and Materials in the US, a standardized agar-block protocol is commonly used in Europe for fungal decay testing [35,36]. In our study, we wanted to explore both methods to better allow the tested fungi to express their full decay potential on ash wood, as many of the fungal species have not been tested on this wood type.

Table 1. Fungal species and strains used for decay studies and their NCBI GenBank accession numbers.

Strain ID	Species	GenBank
EAB 8-34	<i>Sistotrema brinkmannii</i> (Bres.) J. Erikss.	MT777396
EAB 26-1	<i>Hyphodermella rosae</i> (Bres.) Nakasone	MT777404
EAB 37-10	<i>Stereum complicatum</i> (Fr.) Fr.	MT777419
EAB 43-3	<i>Trametes versicolor</i> (L.) Lloyd	MT777401
EAB 49-10	<i>Phlebia acerina</i> Peck	MT777416
EAB 49-12	<i>Irpex lacteus</i> (Fr.) Fr.	MT777397
EAB 49-16	<i>Peniophora cinerea</i> (Pers.) Cooke	MT777398
EAB 56-6	<i>Ganoderma applanatum</i> (Pers.) Pat.	MT777403
EAB 57-12	<i>Irpex lacteus</i> (Fr.) Fr.	MT777397
EAB 58-20	<i>Peniophora gilbertsonii</i> Boidin	MT777400
EAB 60-6	<i>Phlebia radiata</i> Fr.	MT777402
EAB 67-16	<i>Phlebia tremellosa</i> (Schrad.) Nakasone & Burds.	MT777399
EAB 57-8	<i>Peniophora pseudoversicolor</i> Boidin	MT777405

2.1. Inoculum Preparation

Fungal cultures were transferred from slant tubes to fresh malt yeast agar (MYA): 15 g Oxoid malt extract, 15 g of Difco Bacto agar, 2 g of Oxoid yeast extract and 1 L of deionized water. After 2 weeks, mycelial plugs were cut with a sterile 0.4 mm diameter metal borer from the border of the colony, to obtain active mycelium. Two mycelium plugs were used as inoculum per replicate.

2.2. Ash Wood Substrate

Blocks of 2.5 × 2.5 × 1.25 cm were cut out from a sound ash (*Fraxinus* sp.) board, numbered, and dried in an oven (90 °C) for 48 h, and the dry weight was determined for each block. Blocks were then rehydrated to 70%–80% hydration, by keeping blocks under water for 24 h and then autoclaving them inside glass Petri dishes filled with 10 mL deionized water. Two autoclave cycles were run for 45 min at 121 °C (with the cycles 24 h apart). Twelve blocks (replicates) with consecutive numbers were randomly assigned to a treatment. Achieved hydration percentage was evaluated by comparing the dry weight to post-hydration weight for 10 sample blocks not included in the study.

Small sapwood discs (1.0–2.0 cm diam, 0.5–0.8 cm thickness) were obtained by slicing freshly cut healthy green ash branches into discs with a wood saw. Bark was completely removed from discs after a brief autoclave cycle that facilitated the manual procedure. Discs were numbered, dried in an oven (90 °C) for 48 h and the dry weight was determined for each disc. Sapwood discs were rehydrated to 70%–80% hydration, by keeping discs under water for 24 h and then autoclaving them in glass Petri dishes filled with 10 mL of deionized water. Two autoclave cycles were run for 45 min at 121 °C (with the cycles 24 h apart). Twelve autoclaved discs (replicates) were randomly assigned to a treatment.

2.3. Microcosm Preparation

For the soil microcosms, wide-mouth, glass mason jars (473 mL, metal lid) were filled with 100 mL of a homogeneous mix of soil composed of two parts of loam soil, two parts of vermiculite and one part of peat moss, which was moistened with 45 mL of deionized water. Filled, lidded jars were autoclaved twice for 45 min at 121 °C (with the cycles 24 h apart). Twelve jars (replicates) were randomly assigned to each treatment (a combination of fungal strain and ash wood substrate). Jars were opened in a sterile biosafety cabinet and one

autoclaved wood block or sapwood disc was placed on the sterile substrate using sterilized forceps. Two mycelium plugs were transferred from growing cultures and placed on the side of the block or sapwood disc in contact with the soil and the ash substrate (Figure 1A), and jars were closed and sealed with Parafilm®. For negative controls, twelve blocks or sapwood discs were inoculated with two non-inoculated agar plugs (no mycelium). Jars were labeled indicating the treatment (fungal strain) and block or disc number, as well as the date, and kept in clear, plastic bins at room temperature (21 °C–23 °C) for 27 weeks.

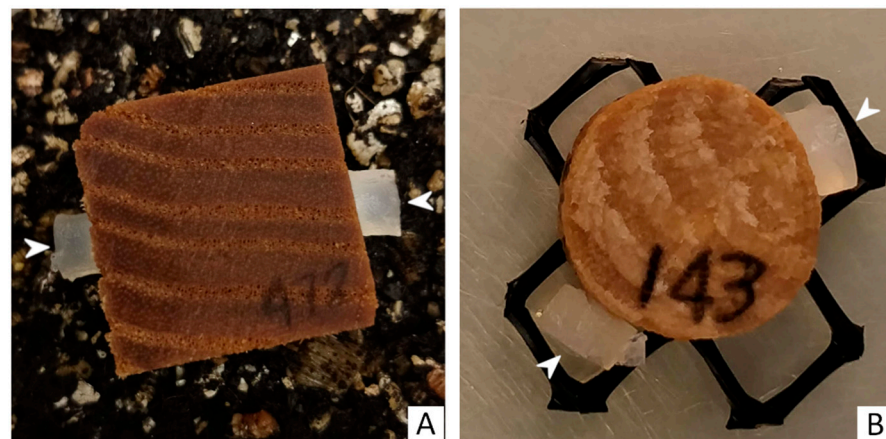


Figure 1. Ash blocks and sapwood discs were used in two studies with soil or agar microcosms. (A) Inoculated ash block in soil microcosm; (B) inoculated ash sapwood disc on plastic mesh in agar microcosm. White arrowheads indicate agar plugs.

For the agar microcosm, an adaptation of methods used by Shilling and Jacobson [38] was used. Extra-deep Petri dishes (10 cm diameter, 2.5 cm deep) were filled with 15 mL of MYA. Pieces of plastic grid mesh (gutter guard, 35 × 35 mm, 2 mm thick) of approximately 3 × 3 cm were cut, thoroughly washed, and autoclaved in glass Petri dishes for 30 min at 121 °C. The agar microcosm was assembled as follows: in a sterile biosafety cabinet one piece of autoclaved plastic mesh grid was placed directly on the media by using sterilized forceps. Then, one autoclaved wood block or sapwood disc was placed on the plastic mesh grid. Two mycelial plugs were transferred from growing cultures and placed on the side of the block or sapwood disc, in contact with the media and the wooden substrate (Figure 1B), and the plate was then closed and sealed with Parafilm®. For negative controls, twelve blocks or sapwood discs were inoculated with two non-inoculated agar plugs (no mycelium). Plates were labeled indicating the treatment (fungal strain) and block or disc number, as well as date, and kept in clear, plastic bins at room temperature for 27 weeks.

After incubation, both the soil and agar microcosms were disassembled. Growing mycelium was carefully removed from blocks and sapwood discs, with special attention to avoid removing any of the wood. All twelve replicates of each treatment were individually placed in small paper envelopes and labelled indicating treatment (fungal strain), experimental setting and block or disc number. Ten replicates of each treatment were then dried (90 °C) for 48 h and weighed. Two replicates of each treatment were stored at −20 °C until preparation for micromorphological studies.

2.4. Loss of Weight Evaluation and Data Analysis

Percentage of weight loss was determined for each replicate from each treatment by comparing the initial dry weight (DW1) with the post-inoculation dry weight (DW2), as follows:

$$\frac{(DW1 - DW2) * 100}{DW1}$$

To compare the percentage of weight loss among the different treatments and the controls, an analysis of variance (ANOVA) was conducted. When the ANOVA was signif-

icant, a Tukey's post hoc multiple comparisons analysis was run to evaluate differences between the different treatments. Statistical analysis and data visualization were performed using the R statistical software (R core team, v.4.22) [39], R packages multcompView [40] and dyplr [41] for data analysis, and tidyverse [42] and ggplot2 [43] for data visualization. Assumptions of linear models, such as normality and homoscedasticity of residuals, were examined through visual examination of residual plots. Weight loss data were expressed as a percentage of the initial weight and data were transformed with the angular transformation (arcsine (square root (weight loss/100))) prior to the ANOVA analysis, to fulfill linearity requirements if needed.

To compare the weight loss produced under the different experimental settings, data from each fungal strain or control, corresponding to either the same microcosm or the same wood substrate, were grouped and a multiple t-test comparison was performed simultaneously with the R package rstatix [44] for data analysis, and tidyverse [42] and ggpubr [45] for data visualization. False discovery rate during the multiple t-test comparison was accounted for by selecting the "BH" p correction method. Weight loss comparisons for each fungal strain were as follows: blocks vs. sapwood discs substrate under soil microcosm, blocks vs. sapwood discs substrate under agar microcosm, soil vs. agar microcosm for the block substrate and soil vs. agar microcosm for the sapwood disc substrate.

2.5. Micromorphological Studies

For micromorphological observations of fungal decay, the samples kept at $-20\text{ }^{\circ}\text{C}$ were cut into smaller segments (wedge shape, approximately $0.2 \times 0.5 \times 0.6\text{ cm}$) and prepared for scanning electron microscopy, following previous methods used by Held et al. [46]. Wooden samples were placed in 24-well plates and infiltrated with 25% Tissue-Freezing Medium (Cat. # TFM-5, General Data, Cincinnati, OH, USA) under vacuum, for 1–2 min. Samples were then mounted on brass stubs, frozen at $-20\text{ }^{\circ}\text{C}$ and sectioned in a cryostat freezing microtome. A transverse cut was made to obtain a clean surface for examination with scanning electron microscopy. Cut samples were then thawed, rinsed several times in water and air-dried, before mounting them on aluminum stubs with carbon adhesive tape followed by coating with gold/palladium (3 nm thickness), using a sputter coater (Cressington 108auto, Ted Pella INC., Redding, CA, USA). Observations of fungal colonization and cell wall degradation were completed with a Hitachi S35N scanning electron microscope.

3. Results

All tested fungal strains showed substrate colonization in microcosms and no mycelium was observed on any of the control treatments. (Figure 2A,E). After 6 months of incubation, several fungal strains showed advanced decay and a significant weight loss under the different experimental settings. The experimental methods used included two wood substrates (blocks or sapwood discs) and two types of microcosms (soil or agar microcosm) (Figures 3–6, Table 2). *Trametes versicolor* (EAB 43-3), *Pe. cinerea* (EAB 49-16), *I. lacteus* (EAB 49-12 and EAB 57-12), *Ph. acerina* (EAB 49-10), *Ph. radiata* (EAB 60-6), *Ph. tremellosa* (EAB 67-16) and *Pe. pseudoversicolor* (EAB 57-8) were among the tested fungi that produced the greatest weight losses. Results from the Tukey's test are shown as box plots, with statistical results on top of the boxes (Figures 3–6). Mean percentage of weight loss and standard deviation for all fungal strains and controls under each experimental setting are presented in Table 2. One replicate of the strain *Si. brinkmannii* (EAB 8-34) in the block-soil microcosm study had to be eliminated, as a small fragment of wood was accidentally removed as mycelia was being removed from the block and was thus, not suitable for weight loss evaluation.

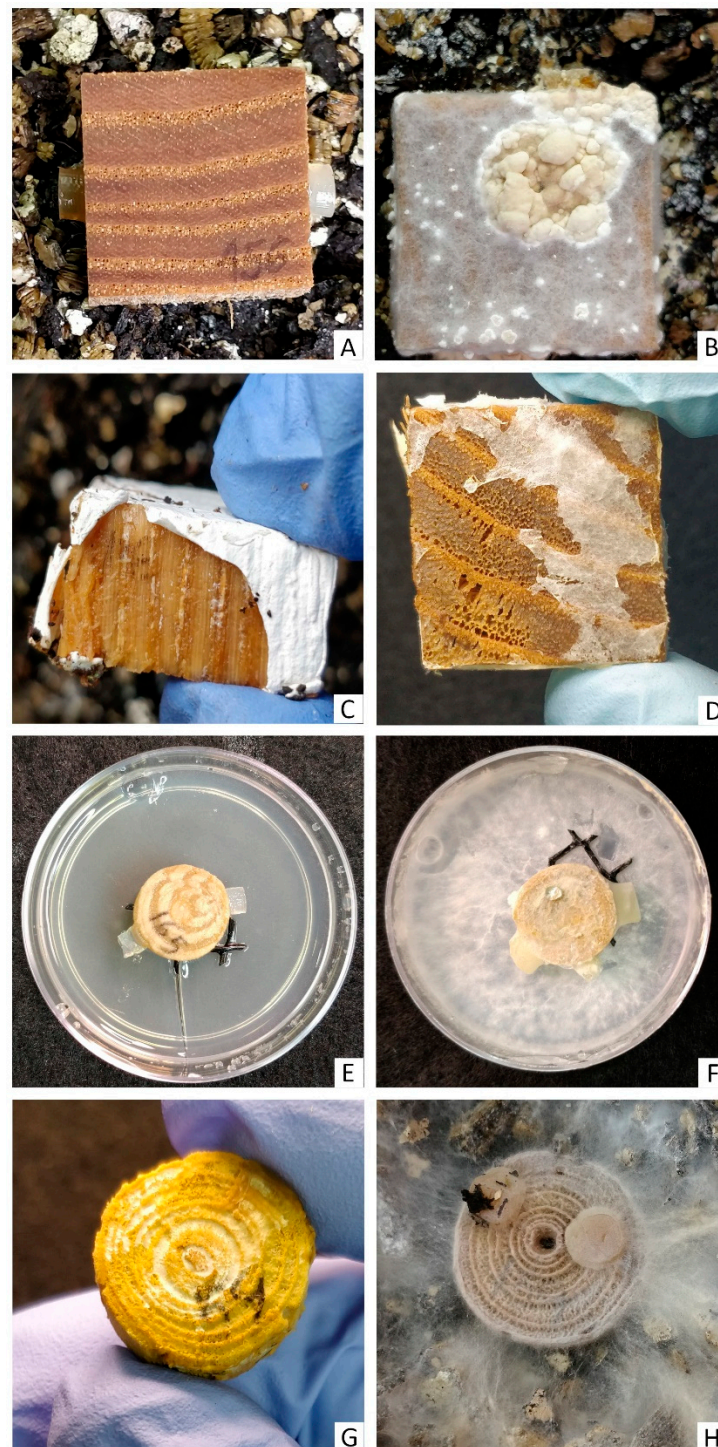


Figure 2. Control and inoculated wood blocks after 6 months of incubation. (A) Control treatment of a wood block from soil microcosm. (B) Growth of *Peniophora cinerea* (EAB 49-16) mycelium on a wood block from a soil microcosm. (C) Removal of mycelium of *Trametes versicolor* (EAB 43-3) from decayed block. (D) Advanced decay of a wood block inoculated with *Peniophora cinerea* (EAB 49-16). (E) Control treatment of sapwood disc in agar microcosm. (F) Growth of *Phlebia radiata* (EAB 60-6) mycelium on sapwood disc in agar microcosm. (G) Advanced decay on sapwood disc inoculated with *Irpex lacteus* (EAB 49-12). (H) Advanced decay of sapwood disc by *Peniophora pseudoversicolor* (EAB 57-8).

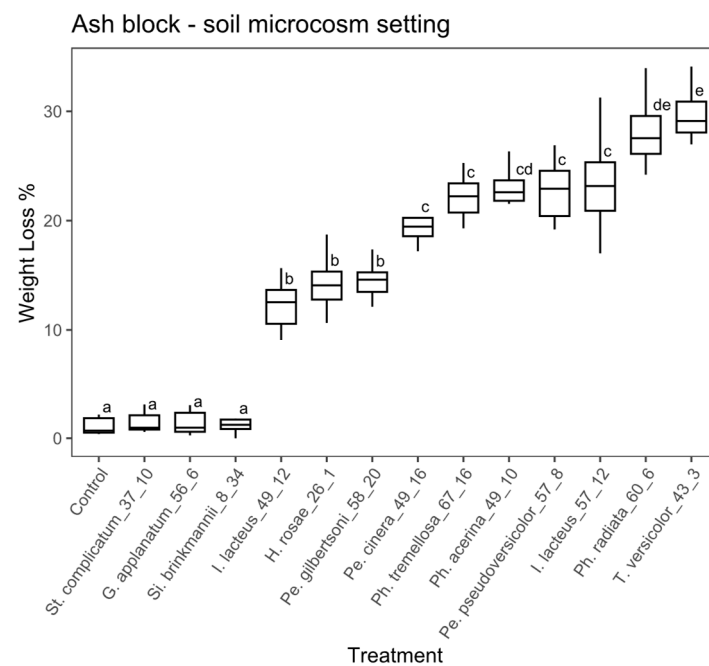


Figure 3. Boxplot of the percentage of weight loss for wooden blocks in the soil microcosm. Different letters represent statistical differences between treatments ($p < 0.01$).

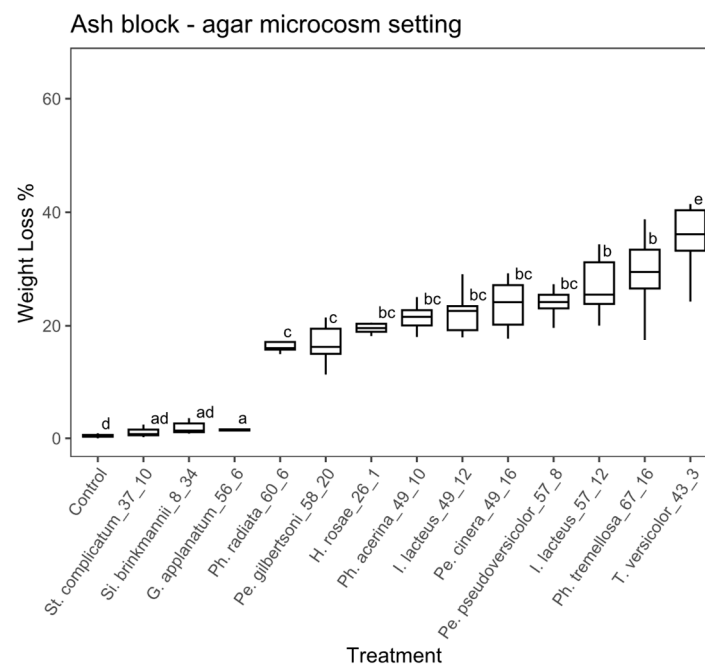


Figure 4. Boxplot of the percentage of weight loss for wooden blocks in the agar microcosm. Different letters represent statistical differences between treatments ($p < 0.01$).

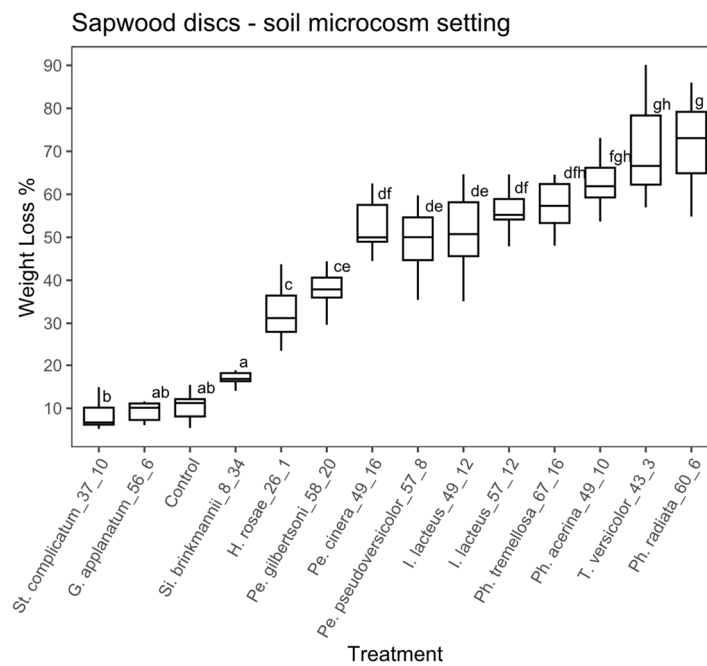


Figure 5. Boxplot of the percentage of weight loss for sapwood discs in the soil microcosm. Different letters represent statistical differences between treatments ($p < 0.01$).

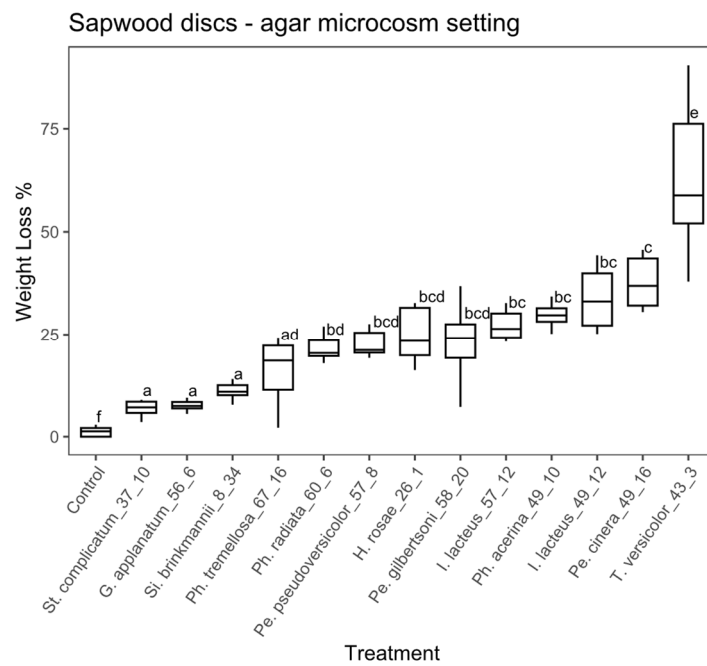


Figure 6. Boxplot of the percentage of weight loss for sapwood discs in the agar microcosm. Different letters represent statistical differences between treatments ($p < 0.01$).

Table 2. Mean percentage of weight loss \pm standard deviation, for all treatments under each experimental setting.

Strain ID	Treatment		Experimental Setting			
	Species		Block Soil	Block Agar	Disc Soil	Disc Agar
—	Control		1.1 \pm 0.7	0.5 \pm 0.3	10.5 \pm 3.2	1.2 \pm 1.2
EAB 8-34	<i>Sistotrema brinkmannii</i>		1.1 \pm 0.7	1.9 \pm 0.8	17.4 \pm 2.5	11.5 \pm 2.5
EAB 26-1	<i>Hyphodermella rosae</i>		14.3 \pm 2.5	19.8 \pm 2.7	33.5 \pm 8.5	25 \pm 6.3

Table 2. Cont.

Strain ID	Treatment Species	Experimental Setting			
		Block Soil	Block Agar	Disc Soil	Disc Agar
EAB 37-10	<i>Stereum complicatum</i>	1.5 ± 0.9	1.1 ± 11.2	8.4 ± 3.3	6.9 ± 1.8
EAB 43-3	<i>Trametes versicolor</i>	29.6 ± 2.2	37.7 ± 0	70.1 ± 11	63.2 ± 18.4
EAB 49-10	<i>Phlebia acerina</i>	23.2 ± 1.8	21.5 ± 2.1	63.7 ± 7.9	29.3 ± 3.8
EAB 49-12	<i>Irpex lacteus</i>	12.2 ± 2.1	22.3 ± 3.5	51 ± 9.6	34.1 ± 7.4
EAB 49-16	<i>Peniophora cinerea</i>	20.5 ± 3.6	23.9 ± 4.2	52.7 ± 6.3	35.4 ± 10.9
EAB 56-6	<i>Ganoderma applanatum</i>	1.9 ± 2.2	3.1 ± 3.7	9.3 ± 2.2	7.5 ± 1.2
EAB 57-12	<i>Irpex lacteus</i>	22.9 ± 5	26.9 ± 5.1	56.2 ± 5.9	27.2 ± 3.5
EAB 57-8	<i>Peniophora pseudoversicolor</i>	22.8 ± 2.7	23.7 ± 2.9	49 ± 7.8	23.7 ± 5.3
EAB 58-20	<i>Peniophora gilbertsoni</i>	14.5 ± 1.5	16.9 ± 3.2	39.1 ± 7.6	23 ± 8.4
EAB 60-6	<i>Phlebia radiata</i>	28.2 ± 3	17 ± 3.4	72.2 ± 9.9	22.1 ± 4.2
EAB 67-16	<i>Phlebia tremellosa</i>	22.7 ± 2.9	27.8 ± 8.7	58.9 ± 9.9	16.3 ± 7.8

3.1. Weight Loss under Different Experimental Settings

Wood block substrate, soil microcosm: the ANOVA analysis for the wood blocks using the soil microcosm showed significant differences among treatments (ANOVA, $F = 205.8$, with 13 and 125 df, $p < 0.01$). The Tukey's test showed that 10 fungal strains significantly differed from the controls (Figure 3). Among the fungal strains that achieved levels of weight loss significantly greater than the control, the percentage of weight loss ranged from 12.2% and 29.6%. *Stereum complicatum* (EAB 37-10), *G. applanatum* (EAB 56-6) and *Si. brinkmannii* (EAB 8-34) did not differ significantly from the control. *Trametes versicolor* (EAB 43-3), *Ph. radiata* (EAB 60-6), *Ph. acerina* (EAB 49-10) and *I. lacteus* (EAB 57-12) achieved the highest weight loss values (29.6%, 28.2%, 23.2% and 22.9%, respectively).

Wood block substrate, agar microcosm: there were significant differences among treatments in the study using wood blocks under the agar microcosm, according to the ANOVA (ANOVA, $F = 104.1$, with 13 and 126 df, $p < 0.01$). A post hoc Tukey's test showed that 10 fungal strains significantly differed from the controls (Figure 4). The percentage of weight loss ranged from 3.1% to 37.7% among the fungal strains with weight loss significantly greater than the control. *Stereum complicatum* (EAB 37-10) and *Si. brinkmannii* (EAB 8-34) did not differ significantly from the control. *Trametes versicolor* (EAB 43-3), *Ph. tremellosa* (EAB 67-16), *I. lacteus* (EAB 57-12) and *Pe. cinerea* (EAB 49-16) achieved the highest weight loss values (37.7%, 27.8%, 26.9% and 23.9%, respectively).

Sapwood discs substrate, soil microcosm: in the case of the sapwood discs using the soil microcosm, the ANOVA analysis also showed significant differences between treatments (ANOVA, $F = 99.41$, with 13 and 126 df, $p < 0.01$). According to the Tukey's test, 10 fungal strains significantly differed from the controls (Figure 5) and among those, the percentage of weight loss ranged from 17.4% to 72.2%. *Si. brinkmannii* (EAB 8-34) and *G. applanatum* (EAB 56-6) did not differ significantly from the control. *Phlebia radiata* (EAB 60-6), *T. versicolor* (EAB 43-3), *Ph. acerina* (EAB 49-10) and *Ph. tremellosa* (EAB 67-16) achieved the highest weight loss values (72.2%, 70.1%, 63.7% and 58.9%, respectively).

Sapwood discs substrate, agar microcosm: the ANOVA analysis for the sapwood discs using the agar microcosm showed that some of the treatments significantly differed between each other (ANOVA, $F = 48.98$, with 13 and 126 df, $p < 0.01$). Thirteen fungal strains were significantly different from the control according to the Tukey's test (Figure 6), with a percentage weight loss ranging from 6.9% to 63.2%. *Trametes versicolor* (EAB 43-3), *Pe. cinerea* (EAB 49-16), *I. lacteus* (EAB 49-12) and *Ph. acerina* (EAB 49-10) achieved the highest weight loss values (63.2%, 35.4%, 34.1% and 29.3%, respectively).

When comparing the experimental settings, significantly greater weight loss was observed among the sapwood discs vs. wood blocks under the soil microcosm for all 13 fungal strains (Figure S1). Under the agar microcosm, nine fungal strains showed significantly more decay among the sapwood discs compared to the wood blocks, and only one showed greater decay for the blocks (Figure S2). When comparing substrates, for the

experiments that used wood blocks, two fungal strains showed significantly more decay under the agar microcosm and only one showed higher decay under the soil microcosm (Figure S3). For the experiments that used sapwood discs as the substrate, ten fungal strains showed significantly more decay under the soil microcosm (Figure S4, Supplementary Materials).

Micromorphological Studies

Scanning electron microscopy (SEM) images from transverse sections of non-decayed wood from the controls showed the typical morphology of sound wood cells. The wood of *Fraxinus* is ring-porous, with earlywood characterized by wide vessels, vascentric parenchyma, fibers and a few smaller vessels in the summer to latewood cells [47–49] (Figure 7A,B).

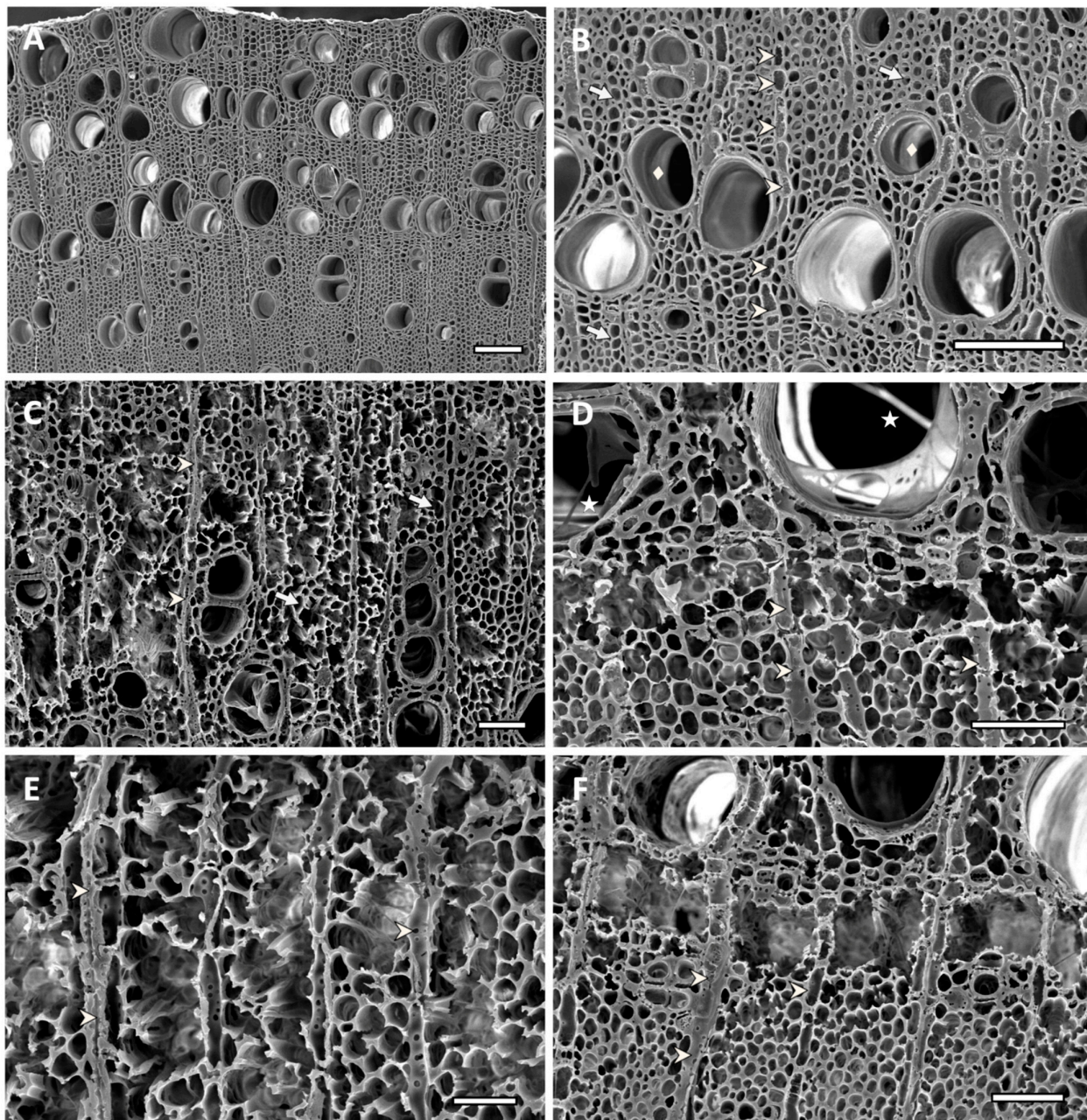


Figure 7. Scanning electron micrographs of transverse sections of ash sapwood disc samples. Arrow indicates fibers, arrowhead indicates ray parenchyma, diamond shape indicates vessels and star shape

indicates mycelium. (A,B) Non-inoculated control showing unaltered fibers and vessels, and the typical morphology of ash sound wood cells (bar = 125 μm). (C) Sample inoculated with *Hyphodermella rosae* (EAB 26-1), showing simultaneous degradation and eroded fibers, with cell walls that were eroded and thinned from the lumen towards the middle lamella. Parenchyma cells, rays and vessels are still recognizable (bar = 50 μm). (D) Simultaneous degradation produced by *Peniophora gilbertsoni* (EAB 58-20), showing thinned walls of fibers, cell wall erosion and loss of fiber structure in some areas, creating localized voids. Mycelia inside the lumen of some high-diameter vessels (bar = 50 μm). (E) Advanced erosion of cell wall from fibers and vessels, produced by simultaneous degradation by *Peniophora pseudoversicolor* (EAB 57-8). Extended voids produced by complete cell wall degradation, parenchyma rays, although somewhat eroded, are still distinguishable (bar = 25 μm). (F) Simultaneous degradation produced by *Irpex lacteus* (EAB 49-12). Advanced localized fiber cell wall erosion causing voids that coalesced, producing holes. Ray parenchyma cells are still distinguishable in areas with coalesced voids (bar = 50 μm).

Samples that had a significant weight loss showed varying degrees of degradation, with areas of extensive decay and almost complete loss of some fiber cell walls for treatments that had over 30% of weight loss (Figures 7 and 8). Wood inoculated with *H. rosae* (EAB 26-1) (Figure 7C), *Pe. gilbertsoni* (58-20) (Figure 7D), *Pe. pseudoversicolor* (57-8) (Figure 7E) or *I. lacteus* (EAB 49-12) (Figure 7F) showed simultaneous degradation of all cell wall components. *Phlebia tremellosa* and *Pe. cinerea* also presented simultaneous degradation of all cell components (not shown). Cell wall erosion occurred with fiber cell walls thinning from the lumen towards the middle lamella. In some areas, all cell walls were degraded, forming voids in the wood. Occasionally, removal of both the secondary walls and the middle lamella, caused voids to coalesce, creating localized holes. In advanced stages of decay, such as those observed on wood inoculated with *T. versicolor* (EAB 43-3) (Figure 8A,B), *Ph. radiata* (EAB 60-6) (Figure 8C) or *Ph. acerina* (EAB 49-10) (Figure 8D–F), the areas that had been extensively attacked created voids that were filled with mycelia. Some ray parenchyma and vessels resisted degradation and were still distinguishable among areas where fibers were completely degraded. Remnants of adjacent fiber and parenchyma cells attached to the vessels could be observed (Figure 8A–F). The significant loss of biomass that occurred in the wood samples inoculated with these white-rot fungi was also evident by the average percentage of weight loss shown in Table 2.

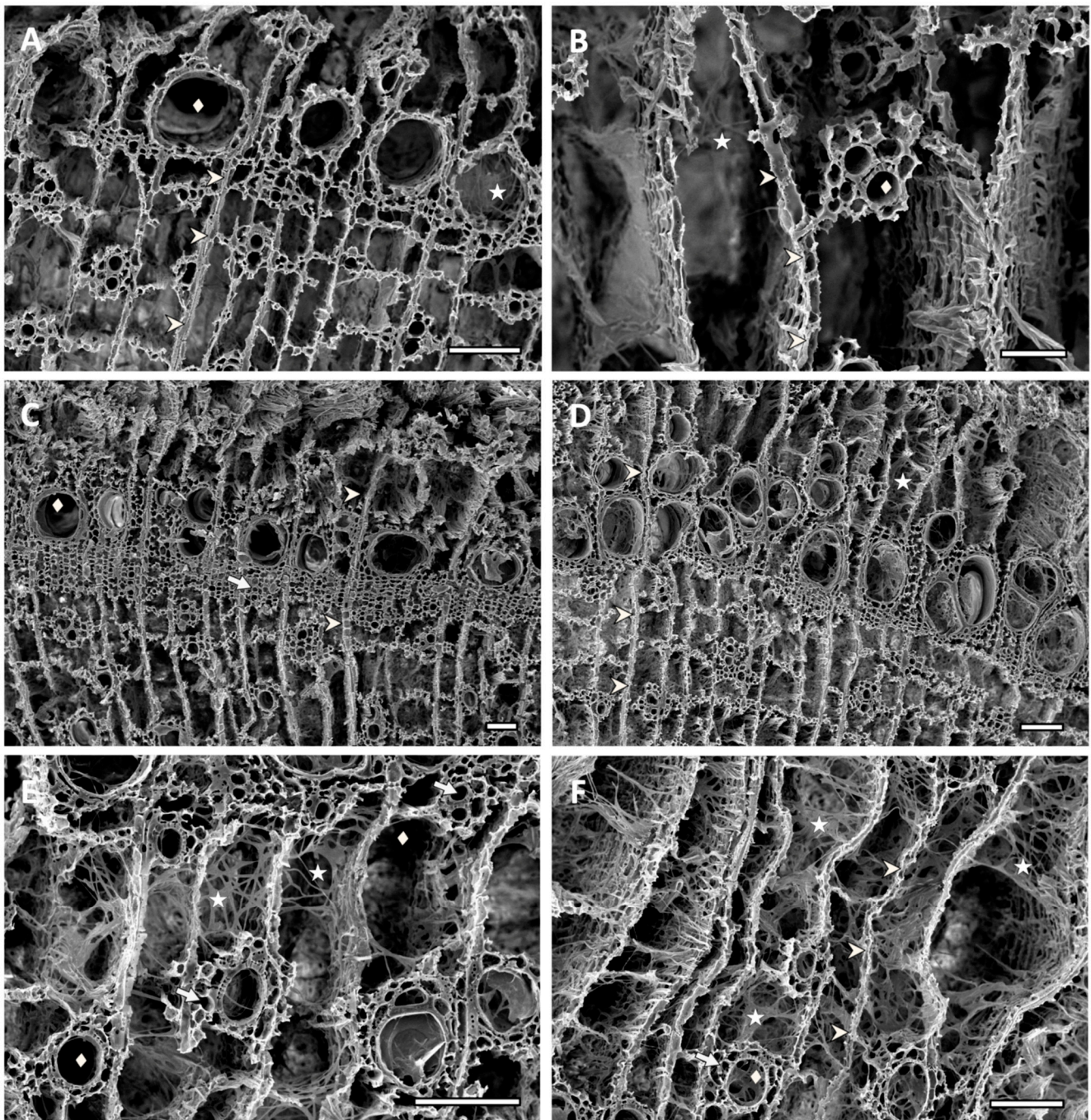


Figure 8. Scanning electron micrographs of transverse sections of ash sapwood disc samples inoculated with white-rot fungi. Arrow indicates fibers, arrowhead indicates ray parenchyma, diamond shape indicates vessels and star shape indicates mycelium. (A,B) Complete loss of fiber cell walls produced by simultaneous degradation by *Trametes versicolor* (EAB 43-3). Coalescence of void-created holes, where remnants of adjacent fiber and parenchyma cells attached to the vessels, can be observed. Ray parenchyma cells were eroded, but still distinguishable. Voids filled with mycelia ((A) bar = 100 μ m, (B) bar = 50 μ m). (C) Extended erosion and thinning of fiber cell walls produced by *Phlebia radiata* (EAB 60-6), and a simultaneous degradation of all cell wall components. Localized collapse of fiber structure and holes produced by coalescing voids. Ray parenchyma cells, vessels and fibers showing erosion are still distinguishable at the center of the image (bar = 100 μ m). (D–F) Extensive decay produced by *Phlebia acerina* (EAB 49-10), showing voids filled with mycelia. Ray parenchyma are eroded, but still distinguishable, and for some remaining vessels, remnants of adjacent fiber and parenchyma cells attached to the vessels can be observed (bar = 100 μ m).

4. Discussion

Highly significant biomass loss and cell wall degradation was observed in the wood samples treated with white-rot fungi associated with EAB galleries, and the decay potential of these species was assessed. Loss of biomass occurred on both types of tested ash wood substrates and for most of the tested fungal strains. This included blocks cut from ash boards and fresh sapwood discs, using two types of microcosms: soil and agar. The strains that produced greater weight loss, such as *T. versicolor* (EAB 43-3), *Pe. cinerea* (EAB 49-16), *I. lacteus* (EAB 49-12 and EAB 57-12), *Ph. acerina* (EAB 49-10), *Ph. radiata* (EAB 60-6), *Ph. tremellosa* (EAB 67-16) and *Pe. pseudoversicolor* (EAB 57-8), also produced significant wood cell wall degradation, which was evident from the micromorphological studies. The more advanced stages of decay produced by *T. versicolor* (EAB 43-3), *Ph. radiata* (EAB 60-6) and *Ph. acerina* (EAB 49-10), had degraded wood cells and extensive voids filled with hyphae. In these treatments only some ray parenchyma cells and vessels resisted degradation. Decay resistance of vessel elements to white-rot fungi has been reported for some hardwood species [50,51]. This has been explained by a combination of different vessel wall structure, as well as a different chemical composition of vessel cell walls. More lignin with a higher guaiacyl lignin type content in vessel walls appears to be a major factor in the resistance of vessels to decay by some white-rot fungi [50,51].

When comparing the different decay experiments, most strains had higher wood degrading capacity on sapwood discs, as compared to the wood blocks. The high proportion or even exclusivity of sapwood tissue in young branch anatomy [52], the low resistance to decay of sapwood compared to heartwood [53,54] and more earlywood cells vs. latewood [55] could explain the higher weight loss on sapwood discs used as substrate during this study. Since sapwood contains simple sugars and other compounds that could be leached out during autoclaving, this is likely the reason that a small weight loss was observed in the untreated sapwood controls, but not in the wood blocks. The sapwood discs used during this study were obtained from young freshly cut healthy branches, whereas the wood blocks were obtained from an ash board commercially available with heartwood. Comparison of the two microcosm experiments showed significant differences in weight loss, with more decay on the agar microcosm when using wood blocks as a substrate. In contrast, most strains showed more decay using the soil microcosm and sapwood discs as the substrate. Both microcosm experiments were equally effective in providing the necessary conditions for the fungal strains to express their decay potential.

After EAB invasion, a significant increase of green ash branch and tree failure was reported by Persad et al. on EAB-infested trees [12]. Despite the species being ranked as intermediate in terms of susceptibility to breakage, EAB-affected trees as early as two years after initial infestation significantly increase their risk of failure and had an increased loss of wood integrity [12]. Ash tree failure associated with EAB infestation has raised great concern because of the risk it poses to tree workers and the public in general. Although the cause of wood strength loss was not determined by Persad et al. [12], the authors observed a significant reduction in the moisture content of EAB wood samples from trees with high infestations compared to those with low or no infestation. A decrease in the high water content of functional sapwood, as well as an increase in oxygen availability, has been identified as a key factor for the colonization of sapwood by decay fungi [51,54,56]. Physical disruption of functional sapwood, due to the serpentine galleries produced by EAB larvae [5], could contribute to the moisture content reduction on the affected area [57], thus providing a suitable microenvironment for decay fungi to develop.

According to Zabel et al. [53], the tree species is an important factor affecting the development of decay. *Fraxinus* spp. and *F. pennsylvanica* in particular, have been classified as having moderate to low resistance to decay [53,58,59]. Held et al. [18] found a community of decay fungi associated with EAB galleries, dominated by white-rot fungi. The dominance of white rot in angiosperms instead of brown-rot fungi has been previously documented [21,60–62]. Among the fungi found by Held et al. (2022) [18], genera such as *Irpex*, *Peniophora* and *Phlebia* appear to be aggressive pioneer colonizers. Species within

those taxa, such as *Pe. pseudoversicolor*, *Ph. acerina*, *Ph. radiata* and *Ph. tremellosa*, were ranked among the top decomposers during this study. Although *T. versicolor* has been previously reported as a pathogen causing dieback and decay on other tree hosts [33,63,64], it was also a very aggressive colonizer, with among the highest loss of biomass in the different experimental settings we report here. Simultaneous removal of all cell wall components (simultaneous white rot) has been previously reported for *T. versicolor* [21,60,63–66] and was observed during this study, as well as with *H. rosae*, *Pe. gilbertsoni*, *Pe. pseudoversicolor*, *Pe. cinerea*, *I. lacteus*, *Ph. radiata*, *Ph. acerina* and *Ph. tremellosa*. Although some of those taxa have been reported as selective white-rotting fungi with preferential lignin removal [67–69], all white-rot fungi that produce a selective lignin removal are likely to also produce a simultaneous rot under certain growth conditions [60,67]. *Sistotrema brinkmannii*, the most abundant decay fungus associated with EAB galleries found by Held et al. [18], did not produce significant weight loss. Although few decay studies have been conducted with *Sistotrema*, it appears to be a poor wood degrader, with very low mass loss [70]. This fungus may just remove nonstructural wood components, such as starch, proteins, triglycerides, etc., or utilize degradation products liberated from wood by other decay fungi. The decay type produced by *S. brinkmannii* remains unclear, with some authors categorizing it as a brown-rot fungus [71,72] and other authors describing it as having an unclear decay type [73]. *Ganoderma applanatum* and *S. complicatum* did not produce significant decay compared to the control, despite *G. applanatum* being reported as a highly efficient white-rot decomposer [61]. This fungus may have a greater role in wood decomposition later in the successional sequence of ash wood decay.

Decay fungi on standing trees may gain access through different strategies: pathogenic mechanisms, reaching the sapwood or heartwood through wounds, or by establishing themselves as endophytic propagules (presumably through natural openings and wounds) which are present within functional sapwood [54]. In their work, Held et al. [18] hypothesized that the lesions produced by EAB larval feeding habits might provide access points for the fungal community observed during their study. Nonetheless, the authors also acknowledge a possible endophytic origin of the fungi, as several of the species were previously reported as endophytes [18,19]. The latent endophytic nature of some decay fungi on standing trees has been widely documented [20,54,74–76] and their ecological role as priority colonizers initiating wood decomposition on the onset of tissue senescence, and thus their effect on community assembly has also been a matter of discussion [20,54,76–78].

To the best of our knowledge, this is the first study to evaluate the decay potential on ash wood samples using Basidiomycota previously isolated from emerald ash-borer-attacked trees, and the first study to identify the cause of the rapid loss of wood strength observed on hazardous EAB-attacked trees. Although the studies were performed under a controlled laboratory environment, they clearly demonstrate the decay capacity of these fungi and their ability to cause significant wood cell wall degradation in a relatively short time if conditions are conducive for decay. Several of the top-ranked decomposers in this study likely play an important role in the loss of wood strength and integrity of EAB-attacked trees. Although *A. planipennis* lacks specialized structures to carry fungal spores such as mycangia, it has been reported that other wood borers that do not have mycangia are able to facilitate the entrance of wood decay fungi by the wounds they produce [79,80].

5. Conclusions

Trees infested with EAB undergo a rapid loss of strength that leads to very hazardous conditions because of their risk of branch and bole failure. Although a drastic reduction of wood moisture has been observed on EAB-attacked trees, a biotic factor has not yet been identified. During this study, several decay fungi associated with EAB galleries inoculated on ash wood in laboratory microcosms achieved high levels of degradation in a relatively short period of time indicating that they can produce an important loss of wood structural strength.

This study provides new information about the degradative ability of several fungal species on ash wood and states the important role that the aggressive pioneer fungi likely play in the observed loss of wood integrity of trees that leads to hazardous tree conditions after EAB infestation.

Supplementary Materials: The following supporting information can be downloaded at: <https://www.mdpi.com/article/10.3390/f14030576/s1>. Figure S1: Block vs. sapwood disc substrate, soil microcosm boxplot; Figure S2: Block vs. sapwood disc substrate, agar microcosm boxplot; Figure S3: Soil vs. agar microcosm, block substrate boxplot; Figure S4: Soil vs. agar microcosm, disc substrate boxplot.

Author Contributions: Conceptualization, R.A.B., S.S. and B.W.H.; methodology, S.S., R.A.B. and B.W.H.; investigation, S.S. and B.W.H.; software, S.S.; formal analysis, S.S.; resources, S.S., B.W.H. and R.A.B.; data curation, S.S. and R.A.B.; writing—original draft preparation, S.S.; writing—review and editing, S.S., R.A.B. and B.W.H.; visualization, S.S.; supervision, R.A.B.; project administration, R.A.B. and B.W.H.; funding acquisition, R.A.B. and B.W.H. All authors have read and agreed to the published version of the manuscript.

Funding: This research was funded by the Minnesota Invasive and Terrestrial Plant and Pests Center, University of Minnesota, and USDA Hatch project MIN22-089.

Institutional Review Board Statement: Not applicable.

Informed Consent Statement: Not applicable.

Data Availability Statement: The data in this study are available within the article.

Acknowledgments: The authors gratefully acknowledge the funding agency and Robert Venette, US Forest Service and Brian Aukema, University of Minnesota and the many city and park personnel in Minneapolis, St. Paul, Plymouth, Duluth, Rochester, Winona, MN, for assistance in sample collection. The authors would also like to express their thanks to Kathryn Bushley for her enriching discussion about the project, and Owen Geier and Ada Fitz for their laboratory assistance.

Conflicts of Interest: The authors declare no conflict of interest. The funders had no role in the design of the study; in the collection, analyses, or interpretation of data; in the writing of the manuscript; or in the decision to publish the results.

References

1. McCullough, D.G. Challenges, Tactics and Integrated Management of Emerald Ash Borer in North America. *For. Int. J. For. Res.* **2019**, *93*, 197–211. [[CrossRef](#)]
2. Aukema, J.E.; Leung, B.; Kovacs, K.; Chivers, C.; Britton, K.O.; Englin, J.; Frankel, S.J.; Haight, R.G.; Holmes, T.P.; Liebhold, A.M.; et al. Economic Impacts of Non-Native Forest Insects in the Continental United States. *PLoS ONE* **2011**, *6*, e24587. [[CrossRef](#)] [[PubMed](#)]
3. Herms, D.A.; Gandhi, K.J.; Smith, A.; Cardina, J.; Knight, K.S.; Herms, C.P.; Long, R.P.; McCullough, D.G. Ecological Impacts of Emerald Ash Borer in Forests of Southeast Michigan. In Proceedings of the 20th US Department of Agriculture Interagency Research Forum on Invasive Species 2009, Annapolis, MD, USA, 13–16 January 2009; McManus, K., Gottschalk, K.W., Eds.; US Department of Agriculture, Forest Service, Northern Research Station: Newtown Square, PA, USA, 2009. General Technical Report NRS-P-51. pp. 36–37.
4. Klooster, W.S.; Gandhi, K.J.; Long, L.C.; Perry, K.I.; Rice, K.B.; Herms, D.A. Ecological Impacts of Emerald Ash Borer in Forests at the Epicenter of the Invasion in North America. *Forests* **2018**, *9*, 250. [[CrossRef](#)]
5. Herms, D.A.; McCullough, D.G. Emerald Ash Borer Invasion of North America: History, Biology, Ecology, Impacts, and Management. *Annu. Rev. Entomol.* **2014**, *59*, 13–30. [[CrossRef](#)] [[PubMed](#)]
6. Kovacs, K.F.; Haight, R.G.; McCullough, D.G.; Mercader, R.J.; Siegert, N.W.; Liebhold, A.M. Cost of Potential Emerald Ash Borer Damage in U.S. Communities, 2009–2019. *Ecol. Econ.* **2010**, *69*, 569–578. [[CrossRef](#)]
7. Sydnor, T.D.; Bumgardner, M.; Subburayalu, S. Community Ash Densities and Economic Impact Potential of Emerald Ash Borer (*Agrilus planipennis*) in Four Midwestern States. *AUF* **2011**, *37*, 84–89. [[CrossRef](#)]
8. Rebek, E.J.; Herms, D.A.; Smitley, D.R. Interspecific Variation in Resistance to Emerald Ash Borer (Coleoptera: Buprestidae) Among North American and Asian Ash (*Fraxinus* Spp.). *Environ. Entomol.* **2008**, *37*, 242–246. [[CrossRef](#)]
9. Rigsby, C.M.; Showalter, D.N.; Herms, D.A.; Koch, J.L.; Bonello, P.; Cipollini, D. Physiological Responses of Emerald Ash Borer Larvae to Feeding on Different Ash Species Reveal Putative Resistance Mechanisms and Insect Counter-Adaptations. *J. Insect Physiol.* **2015**, *78*, 47–54. [[CrossRef](#)]

10. Villari, C.; Herms, D.A.; Whitehill, J.G.A.; Cipollini, D.; Bonello, P. Progress and Gaps in Understanding Mechanisms of Ash Tree Resistance to Emerald Ash Borer, a Model for Wood-boring Insects That Kill Angiosperms. *New Phytol.* **2016**, *209*, 63–79. [[CrossRef](#)]
11. Knight, K.S.; Brown, J.P.; Long, R.P. Factors Affecting the Survival of Ash (*Fraxinus* Spp.) Trees Infested by Emerald Ash Borer (*Agrilus planipennis*). *Biol. Invasions* **2013**, *15*, 371–383. [[CrossRef](#)]
12. Persad, A.B.; Siefer, J.; Montan, R.; Kirby, S.; Rocha, O.J.; Redding, M.E.; Ranger, C.M.; Jones, A.W. Effects of Emerald Ash Borer Infestation on the Structure and Material Properties of Ash Trees. *Arboric. Urban For.* **2013**, *39*, 11–16. [[CrossRef](#)]
13. Jennings, D.E.; Taylor, P.B.; Duan, J.J. The Mating and Oviposition Behavior of the Invasive Emerald Ash Borer (*Agrilus planipennis*), with Reference to the Influence of Host Tree Condition. *J. Pest Sci.* **2014**, *87*, 71–78. [[CrossRef](#)]
14. Cappaert, D.; McCullough, D.G.; Poland, T.M.; Siegert, N.W. Emerald Ash Borer in North America: A Research and Regulatory Challenge. *Am. Entomol.* **2005**, *51*, 152–165. [[CrossRef](#)]
15. Lyons, D.; Jones, G.; Wainio-Keizer, K. Biology and Phenology of the Emerald Ash Borer, *Agrilus planipennis*. In Proceedings of the XV U.S. Department of Agriculture Interagency Research Forum on Gypsy Moth and Other Invasive Species 2004, Annapolis, MD, USA, 13–16 January 2004.
16. Bauer, L.; Haack, R.A.; Miller, D.L.; Petrice, T.R. Emerald Ash Borer Life Cycle. In Proceedings of the Emerald Ash Borer Research and Technology Development Meeting, Port Huron, MI, USA, 30 September–1 October 2003; Mastro, V., Reardon, R., Eds.; U.S. Forest Service, Forest Health Technology Enterprise Team: Morgantown, WV, USA, 2004. FHTET 2004-02.
17. Kolka, R.K.; D’Amato, A.W.; Wagenbrenner, J.W.; Slesak, R.A.; Pypker, T.G.; Youngquist, M.B.; Grinde, A.R.; Palik, B.J. Review of Ecosystem Level Impacts of Emerald Ash Borer on Black Ash Wetlands: What Does the Future Hold? *Forests* **2018**, *9*, 179. [[CrossRef](#)]
18. Held, B.W.; Simeto, S.; Rajtar, N.N.; Cotton, A.J.; Showalter, D.N.; Bushley, K.E.; Blanchette, R.A. Fungi Associated with Galleries of the Emerald Ash Borer. *Fungal Biol.* **2021**, *125*, 551–559. [[CrossRef](#)]
19. Rajtar, N.N.; Held, B.W.; Blanchette, R.A. Fungi from Galleries of the Emerald Ash Borer Produce Cankers in Ash Trees. *Forests* **2021**, *12*, 1509. [[CrossRef](#)]
20. Song, Z.; Kennedy, P.G.; Liew, F.J.; Schilling, J.S. Fungal Endophytes as Priority Colonizers Initiating Wood Decomposition. *Funct. Ecol.* **2017**, *31*, 407–418. [[CrossRef](#)]
21. Eriksson, K.-E.L.; Blanchette, R.A.; Ander, P. *Microbial and Enzymatic Degradation of Wood and Wood Components*; Springer Science & Business Media: Berlin/Heidelberg, Germany, 2012; ISBN 978-3-642-46687-8.
22. Riley, R.; Salamov, A.A.; Brown, D.W.; Nagy, L.G.; Floudas, D.; Held, B.W.; Levasseur, A.; Lombard, V.; Morin, E.; Otilar, R.; et al. Extensive Sampling of Basidiomycete Genomes Demonstrates Inadequacy of the White-Rot/Brown-Rot Paradigm for Wood Decay Fungi. *Proc. Natl. Acad. Sci. USA* **2014**, *111*, 9923–9928. [[CrossRef](#)]
23. Blanchette, R.A. Delignification by Wood-Decay Fungi. *Annu. Rev. Phytopathol.* **1991**, *29*, 381–403. [[CrossRef](#)]
24. Schilling, J.S.; Kaffenberger, J.T.; Liew, F.J.; Song, Z. Signature Wood Modifications Reveal Decomposer Community History. *PLoS ONE* **2015**, *10*, e0120679. [[CrossRef](#)]
25. Anulewicz, A.C.; McCullough, D.; Cappaert, D. Emerald Ash Borer (*Agrilus planipennis*) Density and Canopy Dieback in Three North American Ash Species. *Arboric. Urban For.* **2007**, *33*, 338–349. [[CrossRef](#)]
26. Poland, T.M.; Chen, Y.; Koch, J.; Pureswaran, D. Review of the Emerald Ash Borer (Coleoptera: Buprestidae), Life History, Mating Behaviours, Host Plant Selection, and Host Resistance. *Can. Entomol.* **2015**, *147*, 252–262. [[CrossRef](#)]
27. Tanis, S.R.; McCullough, D.G. Differential Persistence of Blue Ash and White Ash Following Emerald Ash Borer Invasion. *Can. J. For. Res.* **2012**, *42*, 1542–1550. [[CrossRef](#)]
28. Raupp, M.J.; Cumming, A.B.; Raupp, E.C. Street Tree Diversity in Eastern North America and Its Potential for Tree Loss to Exotic Borers. *Arboric. Urban For.* **2006**, *32*, 297–304. [[CrossRef](#)]
29. 2019 Minnesota State Agency Emerald Ash Borer Report | Minnesota Environmental Quality Board. Available online: <https://www.eqb.state.mn.us/2019-minnesota-state-agency-emerald-ash-borer-report> (accessed on 24 October 2022).
30. Community Tree Inventories | The UFOR Nursery & Lab. Available online: <https://trees.umn.edu/outreach/community-tree-inventories> (accessed on 24 October 2022).
31. Coetzee, M.P.A.; Marincowitz, S.; Muthelo, V.G.; Wingfield, M.J. Ganoderma Species, Including New Taxa Associated with Root Rot of the Iconic *Jacaranda mimosifolia* in Pretoria, South Africa. *IMA Fungus* **2015**, *6*, 249–256. [[CrossRef](#)] [[PubMed](#)]
32. Paterson, R.R.M. Ganoderma Disease of Oil Palm—A White Rot Perspective Necessary for Integrated Control. *Crop Prot.* **2007**, *26*, 1369–1376. [[CrossRef](#)]
33. Mang, S.M.; Marcone, C.; Maxim, A.; Camele, I. Investigations on Fungi Isolated from Apple Trees with Die-Back Symptoms from Basilicata Region (Southern Italy). *Plants* **2022**, *11*, 1374. [[CrossRef](#)]
34. Archer, K.; Nicholas, D.D.; Schultz, T.P. Screening of Wood Preservatives: Comparison of the Soil-Block, Agar-Block, and Agar-Plate Tests. *For. Prod. J.* **1995**, *45*, 86.
35. Kuo, C.-J.; Kimsey, M.; Page-Dumroese, D.S.; Kirker, G.; Fu, A.Q.; Cai, L. Investigating Soil Effects on Outcomes of a Standardized Soil-Block Test. *For. Prod. J.* **2022**, *72*, 140–146. [[CrossRef](#)]
36. Wiejak, A.; Francke, B. Testing and Assessing Method for the Resistance of Wood-Plastic Composites to the Action of Destroying Fungi. *Materials* **2021**, *14*, 697. [[CrossRef](#)]

37. Wazny, J.; Cookson, L.J. Comparison of the Agar-Block and Soil-Block Methods Used for Evaluation of Fungitoxic Value of Wood Preservatives. *Folia For. Polonica. Ser. B-Drzew.* **1995**, *25*, 73–82.
38. Schilling, J.S.; Jacobson, K.B. Agar-Block Microcosms for Controlled Plant Tissue Decomposition by Aerobic Fungi. *JoVE* **2011**, *48*, 2283. [[CrossRef](#)]
39. R Core Team. *R: A Language and Environment for Statistical Computing*; R Foundation for Statistical Computing: Vienna, Austria, 2022.
40. Graves, S.; Piepho, H.-P.; Dorai-Raj, L.S. *MultcompView: Visualizations of Paired Comparisons*; R Project: Vienna, Austria, 2019.
41. Wickham, H.; François, R.; Henry, L.; Müller, K. *Dplyr: A Grammar of Data Manipulation*; R Project: Vienna, Austria, 2022.
42. Wickham, H. *Tidyverse: Easily Install and Load the Tidyverse*; R Project: Vienna, Austria, 2022.
43. Wickham, H. *Ggplot2: Elegant Graphics for Data Analysis*; Springer: New York, NY, USA, 2016; ISBN 978-3-319-24277-4.
44. Kassambara, A. *Rstatix: Pipe-Friendly Framework for Basic Statistical Tests*; R Project: Vienna, Austria, 2022.
45. Kassambara, A. *Ggpubr: Ggplot2 Based Publication Ready Plots*; R Project: Vienna, Austria, 2022.
46. Held, B.W.; Blanchette, R.A. Deception Island, Antarctica, Harbors a Diverse Assemblage of Wood Decay Fungi. *Fungal Biol.* **2017**, *121*, 145–157. [[CrossRef](#)] [[PubMed](#)]
47. Bajpai, P. Hardwood Anatomy. In *Biermann's Handbook of Pulp and Paper*; Elsevier: Amsterdam, The Netherlands, 2018; pp. 153–208. ISBN 978-0-12-814240-0.
48. Gartner, B.L. *Plant Stems: Physiology and Functional Morphology*; Physiological Ecology; Academic Press: San Diego, CA, USA, 1995; ISBN 978-0-08-053908-9.
49. Panshin, A.J.; Zeeuw, C.D. *Textbook of Wood Technology: Structure, Identification, Uses, and Properties of the Commercial Woods of the United States and Canada*; McGraw-Hill: New York, NY, USA, 1970; ISBN 978-0-07-048440-5.
50. Blanchette, R.A.; Obst, J.R.; Hedges, J.I.; Weliky, K. Resistance of Hardwood Vessels to Degradation by White Rot Basidiomycetes. *Can. J. Bot.* **1988**, *66*, 1841–1847. [[CrossRef](#)]
51. Schwarze, F.W.M.R. Wood Decay under the Microscope. *Fungal Biol. Rev.* **2007**, *21*, 133–170. [[CrossRef](#)]
52. Thurner, M.; Beer, C.; Crowther, T.; Falster, D.; Manzoni, S.; Prokushkin, A.; Schulze, E.-D. Sapwood Biomass Carbon in Northern Boreal and Temperate Forests. *Glob. Ecol. Biogeogr.* **2019**, *28*, 640–660. [[CrossRef](#)]
53. Zabel, R.A.; Morrell, J.J. Natural Decay Resistance (Wood Durability). In *Wood Microbiology*; Elsevier: Amsterdam, The Netherlands, 2020; pp. 455–470. ISBN 978-0-12-819465-2.
54. Boddy, L. Fungal Community Ecology and Wood Decomposition Processes in Angiosperms: From Standing Tree to Complete Decay of Coarse Woody Debris. *Ecol. Bull.* **2001**, *49*, 43–56. [[CrossRef](#)]
55. Schwarze, F.W.M.R.; Fink, S.; Deflorio, G. Resistance of Parenchyma Cells in Wood to Degradation by Brown Rot Fungi. *Mycol. Prog.* **2003**, *2*, 267–274. [[CrossRef](#)]
56. Boddy, L.; Rayner, A.D.M. Ecological Roles of Basidiomycetes Forming Decay Communities in Attached Oak Branches. *New Phytol.* **1983**, *93*, 77–88. [[CrossRef](#)]
57. Chen, Y.; Ciaramitaro, T.; Poland, T.M. Moisture Content and Nutrition as Selection Forces for Emerald Ash Borer Larval Feeding Behaviour. *Ecol. Entomol.* **2011**, *36*, 344–354. [[CrossRef](#)]
58. Baietto, M.; Wilson, A.D. Relative in Vitro Wood Decay Resistance of Sapwood from Landscape Trees of Southern Temperate Regions. *HortScience* **2010**, *45*, 401–408. [[CrossRef](#)]
59. Scheffer, T.C. Natural Resistance of Wood to Microbial Deterioration. *Annu. Rev. Phytopathol.* **1966**, *4*, 147–168. [[CrossRef](#)]
60. Blanchette, R.A. Degradation of the Lignocellulose Complex in Wood. *Can. J. Bot.* **1995**, *73*, 999–1010. [[CrossRef](#)]
61. Gilbertson, R.L.; Ryvarden, L. *North American Polypores. Vol. 1. Abortiporus-Lindtneria*; Fungiflora A/S: Oslo, Norway, 1986.
62. Gilbertson, R.L.; Ryvarden, L. *North American Polypores Vol. 2. Megasporoporia-Wrightoporia*; Fungiflora A/S: Oslo, Norway, 1987; pp. 437–885.
63. Bari, E.; Nazarnezhad, N.; Kazemi, S.M.; Tajick Ghanbary, M.A.; Mohebbi, B.; Schmidt, O.; Clausen, C.A. Comparison between Degradation Capabilities of the White Rot Fungi *Pleurotus ostreatus* and *Trametes versicolor* in Beech Wood. *Int. Biodeterior. Biodegrad.* **2015**, *104*, 231–237. [[CrossRef](#)]
64. Bari, E.; Daryaei, M.G.; Karim, M.; Bahmani, M.; Schmidt, O.; Woodward, S.; Tajick Ghanbary, M.A.; Sistani, A. Decay of *Carpinus betulus* Wood by *Trametes versicolor*—An Anatomical and Chemical Study. *Int. Biodeterior. Biodegrad.* **2019**, *137*, 68–77. [[CrossRef](#)]
65. Singh, P.; Sulaiman, O.; Hashim, R.; Peng, L.C.; Singh, R.P. Evaluating Biopulping as an Alternative Application on Oil Palm Trunk Using the White-Rot Fungus *Trametes versicolor*. *Int. Biodeterior. Biodegrad.* **2013**, *82*, 96–103. [[CrossRef](#)]
66. Blanchette, R.A. Screening Wood Decayed by White Rot Fungi for Preferential Lignin Degradation. *Appl. Environ. Microbiol.* **1984**, *48*, 647–653. [[CrossRef](#)]
67. Blanchette, R.A.; Reid, I.D. Ultrastructural Aspects of Wood Delignification by *Phlebia (Merulius) Tremellosus*. *Appl. Environ. Microbiol.* **1986**, *52*, 239–245. [[CrossRef](#)]
68. Maillard, F.; Schilling, J.; Andrews, E.; Schreiner, K.M.; Kennedy, P. Functional Convergence in the Decomposition of Fungal Necromass in Soil and Wood. *FEMS Microbiol. Ecol.* **2020**, *96*, fiz209. [[CrossRef](#)]
69. Ortiz, R.; Párraga, M.; Navarrete, J.; Carrasco, I.; de la Vega, E.; Ortiz, M.; Herrera, P.; Jurgens, J.A.; Held, B.W.; Blanchette, R.A. Investigations of Biodeterioration by Fungi in Historic Wooden Churches of Chiloé, Chile. *Microb. Ecol.* **2014**, *67*, 568–575. [[CrossRef](#)]

70. Son, E.; Kim, J.-J.; Lim, Y.W.; Au-Yeung, T.T.; Yang, C.Y.H.; Breuil, C. Diversity and Decay Ability of Basidiomycetes Isolated from Lodgepole Pines Killed by the Mountain Pine Beetle. *Can. J. Microbiol.* **2011**, *57*, 33–41. [[CrossRef](#)] [[PubMed](#)]
71. Potvin, L.R.; Richter, D.L.; Jurgensen, M.F.; Dumroese, R.K. Association of *Pinus banksiana* Lamb. and *Populus tremuloides* Michx. Seedling Fine Roots with *Sistotrema brinkmannii* (Bres.) J. Erikss. (Basidiomycotina). *Mycorrhiza* **2012**, *22*, 631–638. [[CrossRef](#)] [[PubMed](#)]
72. Kowalski, T.; Bilański, P. Fungi Detected in the Previous Year’s Leaf Petioles of *Fraxinus excelsior* and Their Antagonistic Potential against *Hymenoscyphus fraxineus*. *Forests* **2021**, *12*, 1412. [[CrossRef](#)]
73. Schilling, J.S.; Kaffenberger, J.T.; Held, B.W.; Ortiz, R.; Blanchette, R.A. Using Wood Rot Phenotypes to Illuminate the “Gray” Among Decomposer Fungi. *Front. Microbiol.* **2020**, *11*, 1288. [[CrossRef](#)] [[PubMed](#)]
74. Boddy, L.; Griffith, G.S. Role of Endophytes and Latent Invasion in the Development of Decay Communities in Sapwood of Angiospermous Trees. *Sydowia* **1989**, *41*, 41–73.
75. Boddy, L.; Hiscox, J.; Gilmartin, E.C.; Johnston, S.R.; Heilmann-Clausen, J. Chapter 12 Wood Decay Communities in Angiosperm Wood. In *The Fungal Community*; Dighton, J., White, J.F., Eds.; CRC Press: Boca Raton, FL, USA, 2017; pp. 169–190.
76. Gilmartin, E.C.; Jusino, M.A.; Pyne, E.J.; Banik, M.T.; Lindner, D.L.; Boddy, L. Fungal Endophytes and Origins of Decay in Beech (*Fagus sylvatica*) Sapwood. *Fungal Ecol.* **2022**, *59*, 101161. [[CrossRef](#)]
77. Cline, L.C.; Schilling, J.S.; Menke, J.; Groenhof, E.; Kennedy, P.G. Ecological and Functional Effects of Fungal Endophytes on Wood Decomposition. *Funct. Ecol.* **2018**, *32*, 181–191. [[CrossRef](#)]
78. Parfitt, D.; Hunt, J.; Dockrell, D.; Rogers, H.J.; Boddy, L.; Griffith, G.W. Do All Trees Carry the Seeds of Their Own Destruction? PCR Reveals Numerous Wood Decay Fungi Latently Present in Sapwood of a Wide Range of Angiosperm Trees. *Fungal Ecol.* **2010**, *3*, 338–346. [[CrossRef](#)]
79. Jacobsen, R.M.; Kauserud, H.; Sverdrup-Thygeson, A.; Bjorbækmo, M.M.; Birkemoe, T. Wood-Inhabiting Insects Can Function as Targeted Vectors for Decomposer Fungi. *Fungal Ecol.* **2017**, *29*, 76–84. [[CrossRef](#)]
80. Seibold, S.; Müller, J.; Baldrian, P.; Cadotte, M.W.; Štursová, M.; Biedermann, P.H.W.; Krah, F.-S.; Bässler, C. Fungi Associated with Beetles Dispersing from Dead Wood—Let’s Take the Beetle Bus! *Fungal Ecol.* **2019**, *39*, 100–108. [[CrossRef](#)]

Disclaimer/Publisher’s Note: The statements, opinions and data contained in all publications are solely those of the individual author(s) and contributor(s) and not of MDPI and/or the editor(s). MDPI and/or the editor(s) disclaim responsibility for any injury to people or property resulting from any ideas, methods, instructions or products referred to in the content.